Original article

Protection by collagen peptides from walleye pollock skin on bone formation via inhibition of oxidative stress

Feng Liu [a,b,1], Wencheng Wang [c,1], Yunqiu Xia [b], Xuehong Chen [b], Yantao Han [b], Desen Miao [d], Deyan Zhang [d], Hong Lv [e], Desheng Yang [f], Daisong Zhang [a], Heng Zhang [a], Haitao Wang [g], Dong Cheng [h], Chunbo Wang [b,*]

[a] Pharmaceutical Department, Qingdao Hiser Medical Center, Qingdao, China
[b] Medical College, Qingdao University, Qingdao, China
[c] Qingdao Municipal Center for Disease Control and Prevention, Qingdao, China
[d] Qingdao Fusheng Food Company, Qingdao, China
[e] Pathology Department, Qingdao Hiser Medical Center, Qingdao, China
[f] Medical Laboratory, Qingdao Hiser Medical Center, Qingdao, China
[g] Pharmaceutical Department, Qingdao Central Hospital, Qingdao, China
[h] Zibo Academy of Agricultural Sciences, Zibo, China

ARTICLE INFO

ABSTRACT

Background: Collagen peptides (CP) have been shown to protect against osteoporosis. Yet, its mechanism on anti-osteoporosis remains unclear.

Method: Cell viability, levels of alkaline phosphatase (ALP), reactive oxygen species (ROS), malondialdehyde (MDA) and superoxide dismutase (SOD) of hydrogen peroxide (H_2O_2)-induced oxidative stress in Saos-2 cells pretreated with CP were examined. The effect and regulatory of CP on FBXW7-p100-NF-κB axis and the relationship between the molecules were explored by overexpressing FBXW7, silencing p100 or NF-κB in Saos-2 cells. Western blot and RT-PCR were performed to determine the expressions of FBXW7, p100 and NF-κB. Hematoxylin & Eosin (H&E) staining was performed to determine morphological indexes of bone tissues in ovariectomized-induced osteoporosis rats treated with CP.

Result: CP increased cell viability, ALP and antioxidant activities in H_2O_2-induced oxidative stress in Saos-2 cells. Results on cell viability, ALP, antioxidant levels, protein and gene expression levels in FBXW7-overexpressed, p100-silenced and NF-κB-silenced Saos-2 cells indicate that FBXW7, p100 and NF-κB are the key regulators and CP treatment modulates FBXW7-p100-NF-κB axis in Saos-2 cells. In addition, pretreatment and treatment with CP in ovariectomized rats improved osteoporosis.

Conclusion: CP could effectively prevent and alleviate osteoporosis. The protective effect of CP on osteoporosis was achieved in part by inhibiting oxidative damage of osteoblasts and promoting bone formation.

1. Introduction

Osteoporosis, a systemic metabolic disease that is characterized by severe loss of bone mass and progressive bone micro-architectural deterioration which results in the reduction of bone strength and increased bone fragility. Osteoporosis has become a major global health problem due to the aging population and changes in lifestyle habits (Burge et al., 2007).

The pathogenesis of osteoporosis is intricate. Decreased levels of estrogen and the increase of senescence, which are the two major causes of postmenopausal osteoporosis, have been shown to associate with excessive oxidative stress (Baek et al., 2010; Kadenbach et al., 2009). Other risk factors of postmenopausal osteoporosis including smoking, high blood pressure, diabetes mellitus, can also lead to increased oxidative stress level in the body (Altindag et al., 2008; Hamada et al., 2009). Emerging evidence has prompted a paradigm shift from the model centered on estrogen deficiency for involutional osteoporosis to

aging and oxidative stress (Manolagas, 2010). Oxidative stress induced by reactive oxygen species (ROS) could cause imbalance of bone homeostasis and lead to bone metabolic diseases (Almeida and O'Brien, 2013; Cervellati et al., 2014; Hendrickx et al., 2015; Wauquier et al., 2009). Therefore, supplements promoting antioxidant activity may provide a novel approach to prevent and alleviate osteoporosis or other related bone metabolic disorders.

Collagen peptides (CP), as one of the functional polypeptides, has been widely used in food additives, cosmetic makeup products and biomedical materials. Several studies have reported that collagen peptides could promote osteoblast proliferation and differentiation, decreased osteoclast-mediated bone resorption, and improved bone mineral density in ovariectomized mice (Guillerminet et al., 2010; Kim et al., 2013; Liu et al., 2014). Yet, the underlying molecular mechanism of collagen peptides remains unclear.

Pathways such as BMP-Smads, Wnt/β-catenin, Notch, are known to be involved in osteoblast differentiation and bone formation either directly or indirectly through Runx2 or Osterix, which are key transcription factors for osteoblast differentiation. E3 ubiquitin ligase regulates osteoblast differentiation and bone formation by mediating ubiquitination and degradation of Runx2 (Zhu et al., 2017). It has been reported that the SCF (Skp/Cullin/F-box) family E3 ubiquitin ligase Skp2 had a negative impact on Runx2 by promoting its polyubiquitination and proteasome-dependent degradation (Thacker et al., 2016). F-box and WD repeat domain containing 7 (FBXW7) is a target protein recognition component of the SCF E3 ubiquitin ligase complex. Studies on FBXW7 had been focusing on tumor, however, a recent report showed that FBXW7 inhibits bone formation by regulating old astrocyte specifically induced substance expression through ubiquitin-mediated proteasome degradation (Yumimoto et al., 2013). p100 and NF-κB have been shown to regulate osteoblast differentiation (Chang et al., 2009; Soysa et al., 2010). In multiple myeloma cells, the degradation of p100 was promoted by FBXW7, an upstream regulatory factor of p100. Moreover, p100 is an inhibitor of NF-κB (Busino et al., 2012). Therefore, it was proposed that there is a mutual regulation between FBXW7, p100 and NF-κB in osteoblasts. In the present study, H_2O_2-induced oxidative stress in Saos-2 cells and ovariectomized rats were used to explore the anti-osteoporotic mechanism of CP. We investigated the interaction between FBXW7, p100 and NF-κB in Saos-2 cells and whether CP plays a protective role in osteoblast through FBXW7/p100/NF-κB pathway.

2. Materials and methods

2.1. Cell culture and treatment

Human osteoblastic cell line Saos-2 was purchased from the Chinese Academy of Sciences. The cells were cultured in α-MEM with 10% fetal bovine serum, 100 U/ml of penicillin and 100 μg/ml of streptomycin in an incubator at 37 °C with 5% CO_2.

Saos-2 cells were pretreated with or without CP (Qingdao Fusheng Food Co., Ltd., China) for 48 h before exposing to 300 μM H_2O_2 (Sigma-Aldrich) for 6 h. H_2O_2 was used as exogenous generator of ROS whereas N-acetyl-ʟ-cysteine (NAC, 1 mM) was the positive control in the study.

2.2. Assays of cell viability

The MTT assay was used to determine cell viability. Briefly, the cells were incubated with 100 μl of medium supplemented with 10 μl of MTT solution (5 mg/ml, Sigma-Aldrich) per well at 37 °C

for 4 h after washing the cells twice with phosphate buffered saline. Next, DMSO was added and the plates were shaken for 10 min to dissolve the formazan products. The absorbance of each well was determined by a microplate reader at 570 nm. The cell viability of the control group was defined as 100%.

2.3. Assays of malondialdehyde (MDA), superoxide dismutase (SOD) and alkaline phosphatase (ALP)

MDA, SOD and ALP levels were measured by detection kits (Nanjing Jiancheng Bioengineering Institute, China) according to the manufacturer's instructions. Total protein concentrations were determined using BCA protein assay (Beyotime Biotechnology, China). The absorbance of each sample was normalized against the protein concentration.

2.4. Intracellular reactive oxygen species (ROS) measurement

The intracellular ROS expression level was determined using the ROS assay kit (AAT Bioquest Inc., USA). Briefly, 100 μl of Amplite™ ROS Green working solution was added and the cells were incubated for 1 h at 37 °C with 5% CO_2. All treatment groups except for the normal control group were treated with or without CP (800 μg/ml) and H_2O_2. The fluorescence was detected using a multi-detection microplate reader at 490 nm excitation and 525 nm emission.

2.5. Quantitative real-time polymerase chain reaction (qRT-PCR)

Total RNA was extracted using TRIzol reagent (Invitrogen). The single-stranded cDNA was synthesized using the Fast Quant RT kit (TIANGEN Biotechnology, China). The qRT-PCR was performed using Superreal PreMix Plus (SYBR Green) with the 7300 Real-time PCR System (Applied Biosystems). The expression of target genes FBXW7, p100 and NF-κB were normalized to the reference gene GAPDH. The $2^{-\triangle\triangle}Ct$ method was applied to calculate the relative gene expression. The primers used in the study were as follows: FBXW7, 5′-CCGTGTTTGGGATGTG GAGA-3′ (sense) and 3′-CCCCCACTCTCCAATGTGAC-5′ (antisense); p100, 5′-CTACTCGAC TACGGCGTCAC-3′ (sense) and 3′-GAGTCTCCATGCCGATCC AG-5′ (antisense); NF-κB, 5′-CCAGACCAACAACAACCCCT-3′ (sense) and 3′-GCCTGGTCCCGTGAAATACA-5′ (antisense); GAPDH, 5′-GAGAAGGCTGG GGCTCAT TT-3′ (sense) and 3′-AGTGTGGC ATGGACTGTGG-5′ (antisense).

2.6. Western blotting

The western blotting procedure was performed as previously described with slight modifications (Liu et al., 2016). Briefly, the proteins were separated by SDS-PAGE electrophoresis, transferred onto polyvinylidene fluoride membranes and incubated with the antibodies: anti-FBXW7 (Abcam), anti-p100 (Thermo), anti-NF-κB (Abcam), and anti-β-actin (Abcam). The protein bands were visualized with the ECL Western Blotting kit (Shenggong Bioengineering, China) and quantified using Quantity One analysis software (Bio-Rad, UK).

2.7. Construction and transfection of plasmids

FBXW7 overexpression plasmids, p100 interference plasmids, NF-κB interference plasmids, and their respective negative control plasmids were all constructed by Shanghai Biotech Engineering Co., Ltd. (China). Plasmids were transfected using Lipofectamine 2000 (Invitrogen). Expression of FBXW7, p100, and NF-κB mRNA and protein levels were analyzed by qRT-PCR and western blotting, respectively.

2.8. Animals and experimental design

One hundred 8-week-old Sprague-Dawley female rats were obtained from the Experimental Animal Center of the Lu Kang Pharmaceutical Co., Ltd. (Shandong, China). The rats were housed in a well-ventilated room at 24 ℃ with a 12 h/12 h light/dark cycle and were given free access to food and water. The animals were randomly divided into five groups: sham surgery group (SHAM), ovariectomized group (OVX), CP pre-protection group (CP-P), low concentration CP group (CP-L) and high concentration CP group (CP-H).

The rats underwent sham surgery or bilateral ovariectomy at the age of 12 weeks via abdominal incision under general anesthesia. From the age of 18 weeks, rats in the CP-L and CP-H groups were daily intragastrically administered with CP at a concentration of 0.5 or 1.0 g/kg/d for 17 weeks while the OVX and SHAM groups were given an equivalent volume of saline. Unlike other groups, the rats in the CP-P group were administered intragastrically with CP at a dose of 1 g/kg/d from the age of 9 weeks for 26 weeks, except for the 3 days after ovariectomy.

2.9. Histomorphometric analyses

The right proximal tibia of each animal was fixed with 4% paraformaldehyde, processed for decalcification in 10% EDTA-2Na and embedded in paraffin following standard procedures. Sections were stained with hematoxylin-eosin (H&E). The images were captured using Olympus BX60 light microscope (Japan) and analyzed using ImageJ 1.48v software (National Institutes of Health, USA).

2.10. Statistical analyses

Statistical analyses were performed using SPSS version 17.0 (SPSS Inc., USA). Data were described as means ± standard deviation (SD). All data were analyzed using a one-way analysis of variance (ANOVA) with a Tamhame's multiple comparison post hoc test. Statistical significance was defined as $p < 0.05$.

3. Results

3.1. Protective effects of CP on H_2O_2-induced cytotoxicity in Saos-2 cells

The concentration-dependent effects of CP on Saos-2 cell viability and H_2O_2-induced cell death were first examined. As shown in Fig. 1A, CP did not exhibit cytotoxic effect at concentration ≤1000 μg/mL under normal condition. Instead, it significantly increased Saos-2 cell viability at concentrations range from 200 to 1000 μg/mL. With H_2O_2 treatment, the cell viability was significantly decreased ($p < 0.01$, Fig. 1B). Treatment with CP significantly protected Saos-2 cells against H_2O_2-induced cell injury at concentrations of 400 and 800 μg/mL but not 200 μg/mL (Fig. 1B). These results suggest that CP promotes cell viability and suppresses H_2O_2-induced cell death.

3.2. CP reversed H_2O_2-induced inhibition of ALP activity in Saos-2 cells

ALP is a marker at the early stage of osteoblast differentiation and osteogenic activity. As shown in Fig. 1C, H_2O_2 markedly decreased ALP activity whereas CP attenuated the loss of ALP activity induced by H_2O_2 in a concentration-dependent manner ($p < 0.05$, CP200 versus H_2O_2; $p < 0.01$, CP400/CP800

versus H_2O_2), suggesting that CP promotes osteogenic differentiation.

3.3. CP scavenged H_2O_2-induced ROS and MDA productions, and promoted SOD activity in Saos-2 cells

Assessment of the antioxidant activity of CP showed that H_2O_2 significantly increased the production of ROS (Fig. 1D) and MDA (Fig. 1E) while inhibiting the activity of SOD (Fig. 1F). In cells pre-incubated with CP, the levels of ROS (Fig. 1D) and MDA (Fig. 1E) were suppressed in a concentration-dependent manner, whereas SOD (Fig. 1F) activity significantly increased as compared with the H_2O_2-treated group. These data revealed that CP could attenuate oxidative stress injury induced by H_2O_2.

3.4. CP attenuated H_2O_2-induced oxidative stress injury by inhibiting FBXW7/p100/NF-κB pathway

As shown in Fig. 2A, H_2O_2 increased the mRNA expression of FBXW7, suggesting that H_2O_2 induces oxidative stress damage through FBXW7. The elevated expression of FBXW7 was significantly reversed by CP. In addition, CP treatment at concentrations 400 and 800 μg/mL showed a significant reversal effect on the mRNA expression of NF-κB (CP400/CP800 versus H_2O_2, $p < 0.01$, Fig. 2B) and p100 (CP400/CP800 versus H_2O_2, $p < 0.01$, Fig. 2C) induced by H_2O_2.

To further explore the mechanism of CP, Saos-2 cell lines overexpressing FBXW7, silencing NF-κB or silencing p100 were established. Their proteins and mRNAs expression levels were examined by western blotting (Fig. 3A) and qRT-PCR (Fig. 3B), respectively. Overexpression of FBXW7 down-regulated the expression of p100 and up-regulated the expression of NF-κB. Interestingly, CP significantly suppressed FBXW7 and NF-κB and promoted p100 expression in Saos-2 cells, thereby reversing the effect of H_2O_2 and overexpressed FBXW7 in cells (Fig. 3C). In addition, silencing of p100 upregulate the expression of NF-κB (Fig. 3D). These data strongly suggest that a mutual regulatory relationship between FBXW7, p100, and NF-κB and that FBXW7 is an upstream regulatory factor of p100 and NF-κB while p100 is a negatively regulator of NF-κB.

Further examination showed that the effects of CP on cell viability, ALP and ROS were attenuated by overexpressing FBXW7 or silencing p100 (Fig. 1B, C, D). These results further demonstrated that the effect of CP via FBXW7/p100/NF-κB axis and that FBXW7 is a key factor in this pathway.

3.5. CP improved osteoporosis in ovariectomized rats over time

To evaluate the effect CP on oxidative stress injury *in vivo*, ovariectomized rats as a model of osteoporosis was examined. Six weeks after ovariectomy, we observed decreased in trabecular number (Tb.N) and trabecular thickness (Tb.Th), increased trabecular separation (Tb.Sp), and interrupted continuity of trabecular meshwork in the OVX group as compared to the SHAM group (data not shown), indicating that the pathological model of osteoporosis was successfully established. Twenty-three weeks after ovariectomy (35-week-old rats), the bone tissue microstructure of the OVX rats were severely damaged, the number of trabeculae and the thickness of the trabeculae were further reduced, and the trabecular meshwork disappeared. Compared with the OVX group, all CP-treated groups significantly increased Tb.N, decreased Tb.Sp, and improved the integrity of the trabecular meshwork connection integrity to different extents ($p < 0.05$, Fig. 4).
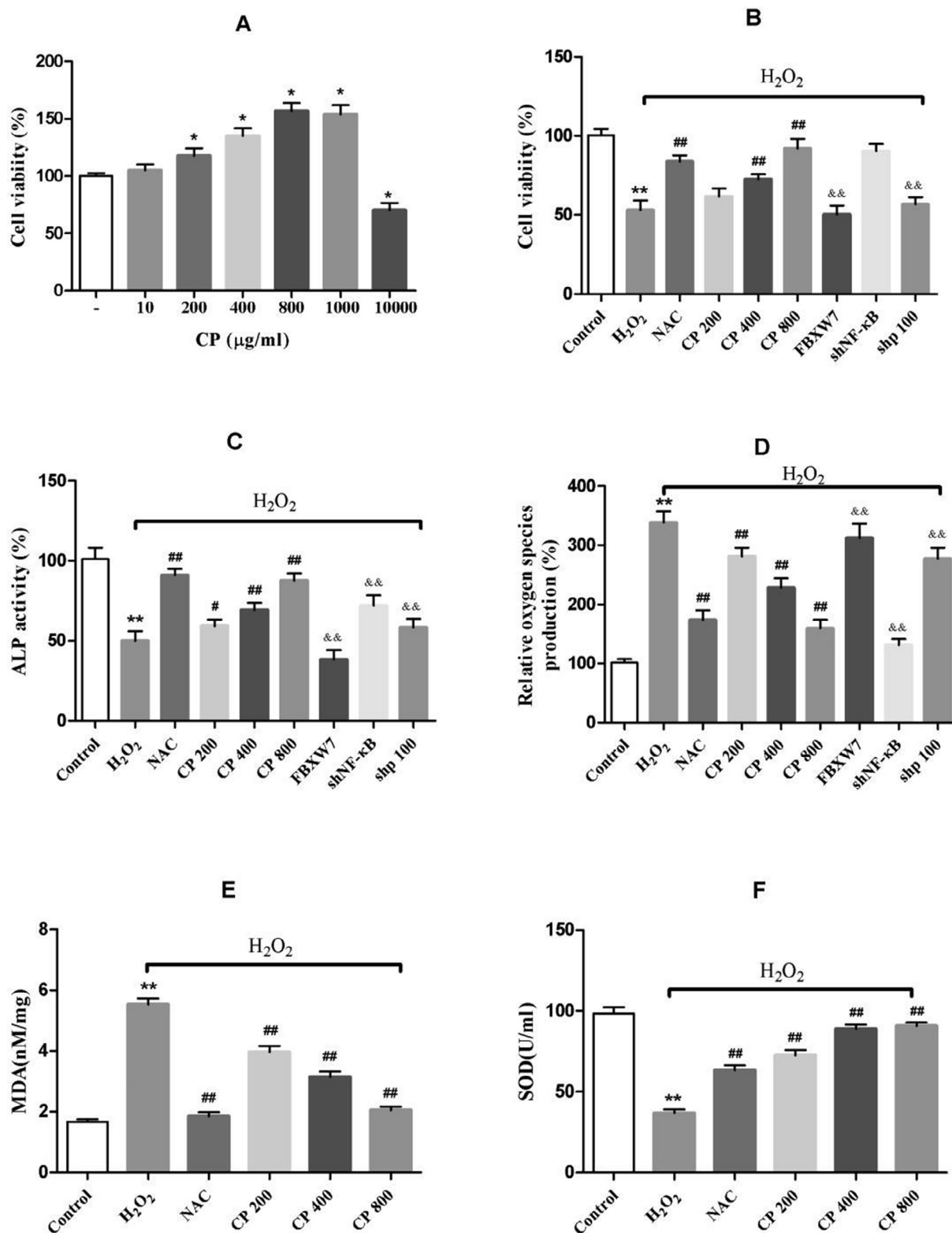
Fig. 1. Effect of CP on cell viability, ALP activity and antioxidant levels in H_2O_2-induced oxidative stress in Saos-2 cells. (A) Effects of CP on the cell viability (B, C, D) Effects of H_2O_2, CP, overexpressed FBXW7, p100 and NF-κB silencing on cell viability, ALP activity, and ROS levels in Saos-2 cells. (E, F) Effects of H_2O_2, and CP on MDA productions and SOD activity in Saos-2 cells. NAC is the positive control. Data shown represent the means ± SD. *$p < 0.05$ and **$p < 0.01$ vs. control group, #$p < 0.05$ and ##$p < 0.01$ vs·H_2O_2 group, and &$p < 0.05$ and &&$p < 0.01$ vs. CP (800 μg/ml) group.
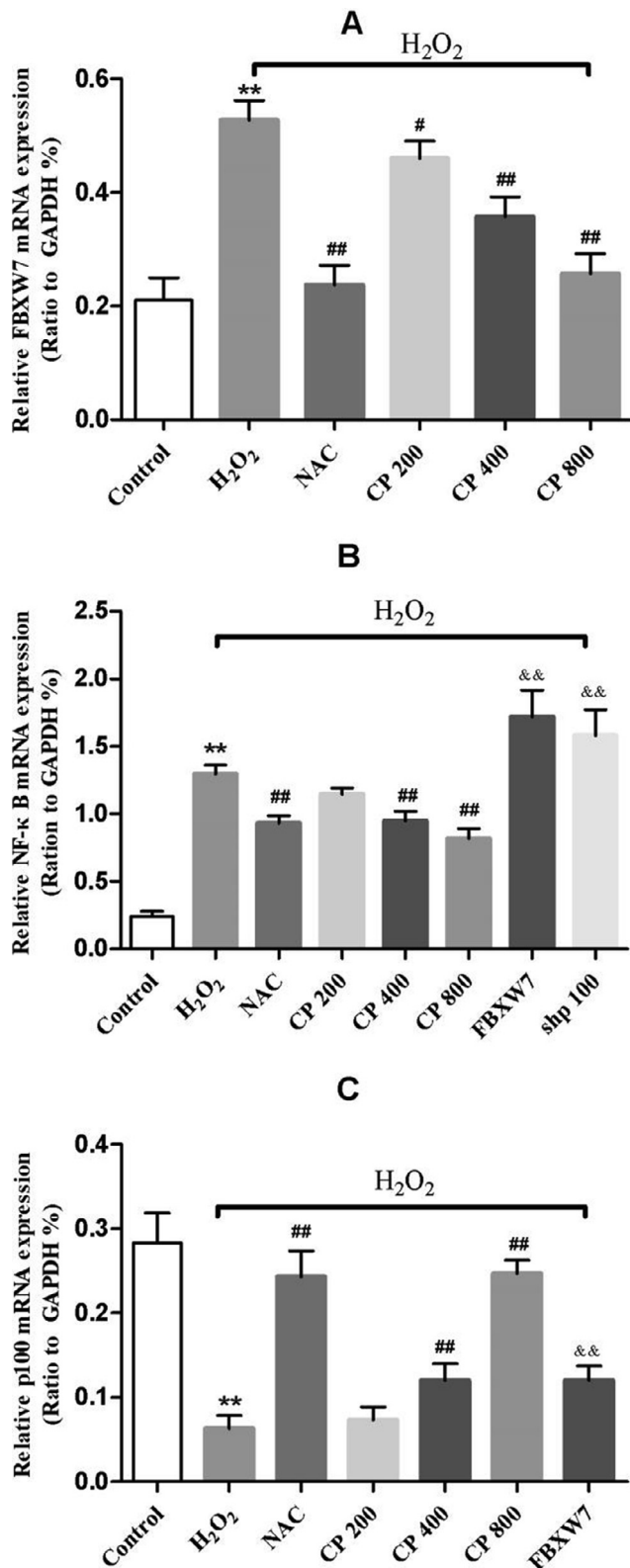
Fig. 2. qRT-PCR analysis of mRNA expression of (A) FBXW7 (B) NF-κB (C) p100 in Saos-2 cells treated with and without overexpressed FBXW7, p100 silencing, H_2O_2 and CP. Data shown represent the means ± SD. $*p < 0.05$ and $**p < 0.01$ vs. control group, $\#p < 0.05$ and $\#\#p < 0.01$ vs. H_2O_2 group, and $\&p < 0.05$ and $\&\&p < 0.01$ vs. CP (800 µg/ml) group.

4. Discussion

Oxidative stress has been identified as important factor in the pathogenesis of osteoporosis caused by aging and estrogen deficiency (Baek et al., 2010). Several studies have reported that H_2O_2-induced oxidative stress increased intracellular ROS levels and inhibited the proliferation and differentiation of osteoblast, which was significantly improved by giving substances with antioxidant properties such as NAC and Rb2 (Bai et al., 2004; Ueno et al., 2011; Huang et al., 2014). Our study demonstrated that CP derived from walleye pollock skin showed excellent antioxidant activity. CP significantly attenuated H_2O_2-induced up-regulation of MDA and ROS, and down-regulation of SOD in a dose-dependent manner. In addition, CP promoted cell proliferation and osteogenic differentiation, characterized by increased cell viability and ALP activity. Bone histomorphology also revealed that CP increased Tb.N and decreased Tb.Sp over time, which partly improved the integrity of the trabecular meshwork structure, especially in CP pretreated rats. Therefore, CP has a certain degree of effectiveness in preventing osteoporosis by protecting osteoblasts from oxidative damage.

We noted a higher expression of FBXW7 in oxidatively injured Saos-2 cells in this study. Interestingly, pretreatment with different concentrations of CP reversed this effect. Further examination revealed that overexpression of FBXW7 impacts cell viability, ALP activity and ROS levels. Study found that depletion of FBXW7 promoted the differentiation of mouse C2C12 mesenchymal cells into osteoblasts (Yumimoto et al., 2013). Our study demonstrated that overexpression of FBXW7 inhibited osteoblast viability and the ALP activity is in line with the previous study showing that FBXW7 is a pivotal factor for osteoblast regulation.

Our results showed that NF-κB was highly expressed whereas p100 levels was low in oxidatively injured Saos-2 cells. Overexpression of FBXW7 significantly up-regulated the expression of NF-κB while inhibiting the expression of p100. In addition, result of silencing of NF-κB reminiscent to the observation in overexpressing FBXW7 which significantly increased cell viability and ALP activity, and reduced ROS production. These further suggest that effect of FBXW7 is mediated by regulating NF-κB. We also found p100 could regulate the expression of NF-κB negatively and alter the cell viability, ALP activity and ROS production. These results suggest that FBXW7, p100 and NF-κB are involved in the regulation of H_2O_2-induced Saos-2 cells by CP. FBXW7 could act as an upstream regulator of p100 and NF-κB and regulate antioxidant activities in the cells.

Previous report showed that bone mineral density was significantly reduced in p100-deficient mice (Soysa et al., 2010). Furthermore, ALP activity and Smad phosphorylation decreased in the primary osteoblasts of p100-deficient mice, and p100 accumulation promoted osteogenic differentiation and *in vivo* osteogenesis in aly/aly mice (Seo et al., 2012). On the other hand, inactivation of NF-κB has been shown to enhance osteoblastic differentiation *in vitro* and bone formation *in vivo* (Jimi and Fukushima, 2016). Selective inhibition of NF-κB blocked the inhibitory effect of TNF-α on BMP2-induced osteoblast differentiation. In addition, inhibition of NF-κB promoted bone formation and improved bone mass loss in ovariectomized mice (Alles et al., 2010; Yamazaki et al., 2009). Our study provides additional evidence that p100 positively regulates osteoblast differentiation and bone formation whereas NF-κB regulates them negatively.

In summary, CP reversed the dysfunction of osteoblasts induced by oxidative stress and protected against osteoporosis
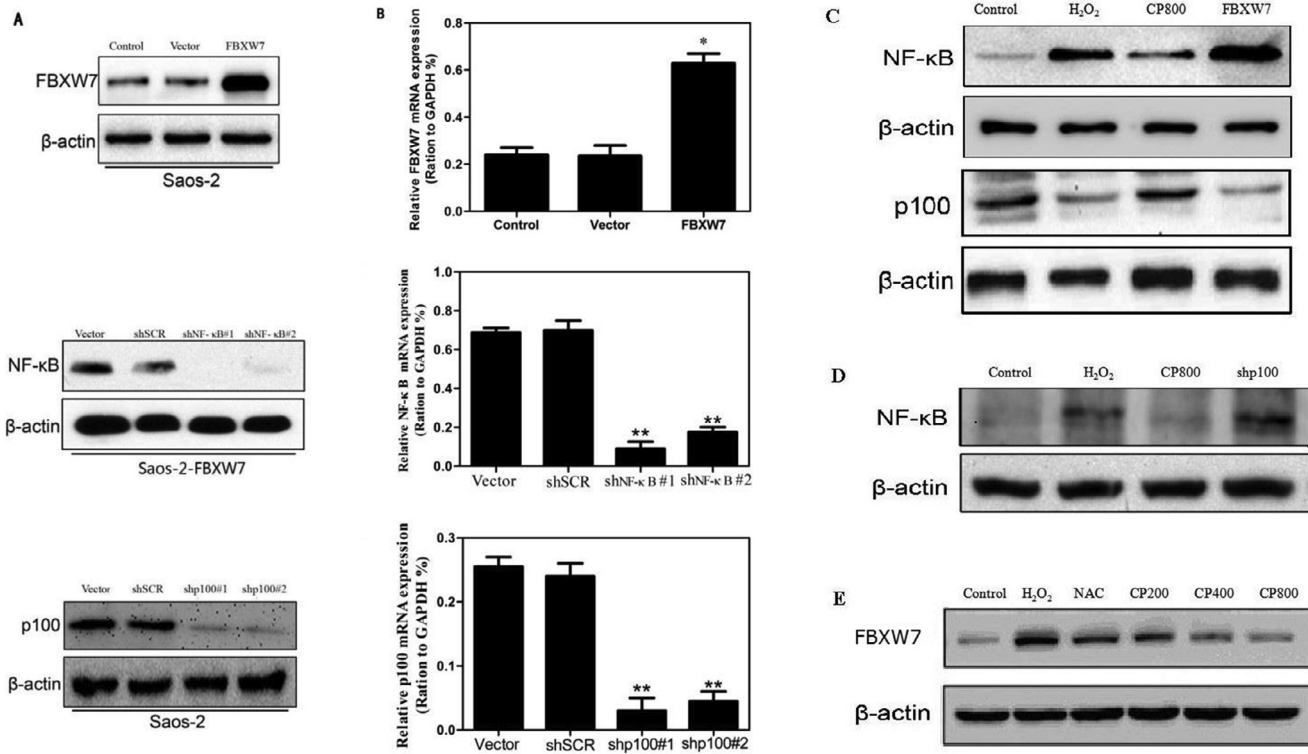
Fig. 3. The mRNA and protein expression levels of FBXW7, p100 and NF-κB were detected by qRT-PCR and Western Blot, respectively. (A, B) Efficiency of overexpressing and silencing of the genes. (C–E) FBXW7 regulates expression levels of p100 and NF-κB. p100 negatively regulate NF-κB protein expression. The values shown represent the means ± SD. *p < 0.05 and **p < 0.01 vs. vector control.
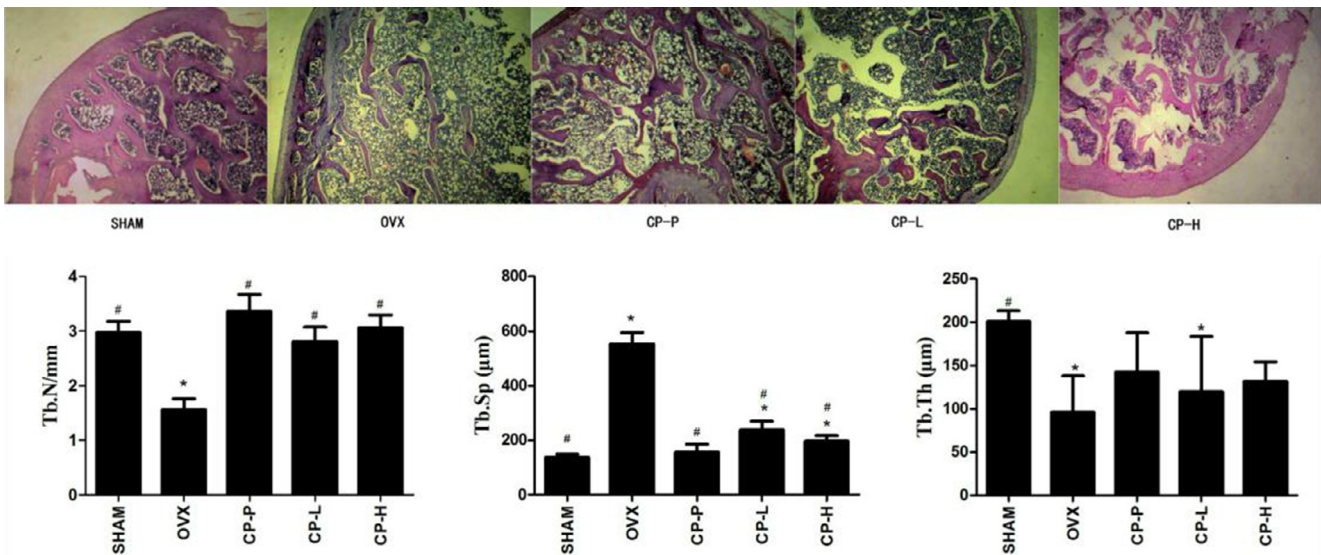

Fig. 4. Representative images of H&E staining (4× magnification) and histomorphometric analyses of the right tibias of 35-week-old ovariectomized rats treated with low concentration CP (CP-L), high concentration CP (CP-H) or pretreated with CP (CP-P). The experiments were repeated three times. Data are expressed as means ± SD. *p < 0.05, vs SHAM group, #p < 0.05, vs. OVX group.

due to oxidative stress and estrogen deficiency. Our study suggests that the protective effect of CP is not only due to its antioxidant activity, but also due to its ability to modulate osteogenic differentiation factors and FBXW7/p100/NF-κB pathway.

Declaration of Competing Interest

The authors declare that they have no known competing financial interests or personal relationships that could have appeared to influence the work reported in this paper.

Acknowledgments

References

Alles, N., Soysa, N., Hayashi, J., Khan, M., Shimoda, A., Shimokawa, H., Ritzeler, O., Akiyoshi, K., Aoki, K., Ohya, K., 2010. Suppression of NF-kappaB increases bone formation and ameliorates osteopenia in ovariectomized mice. Endocrinology 151, 4626–4634.

Almeida, M., O'Brien, C.A., 2013. Basic biology of skeletal aging: role of stress response pathways. J. Gerontol. A: Biol. Sci. Med. Sci. 68, 1197–1208.

Altindag, O., Erel, O., Soran, N., Celik, H., Selek, S., 2008. Total oxidative/anti-oxidative status and relation to bone mineral density in osteoporosis. Rheumatol. Int. 28, 317–321.

Baek, K.H., Oh, K.W., Lee, W.Y., Lee, S.S., Kim, M.K., Kwon, H.S., Rhee, E.J., Han, J.H., Song, K.H., Cha, B.Y., Lee, K.W., Kang, M.I., 2010. Association of oxidative stress with postmenopausal osteoporosis and the effects of hydrogen peroxide on osteoclast formation in human bone marrow cell cultures. Calcif. Tissue Int. 87, 226–235.

Bai, X.C., Lu, D., Bai, J., Zheng, H., Ke, Z.Y., Li, X.M., Luo, S.Q., 2004. Oxidative stress inhibits osteoblastic differentiation of bone cells by ERK and NF-kappaB. Biochem. Biophys. Res. Commun. 314, 197–207.

Burge, R., Dawson-Hughes, B., Solomon, D.H., Wong, J.B., King, A., Tosteson, A., 2007. Incidence and economic burden of osteoporosis-related fractures in the United States, 2005–2025. J. Bone Miner. Res. 22, 465–475.

Busino, L., Millman, S., Scotto, L., Kyratsous, C., Basrur, V., O'Connor, O., Hoffmann, A., Elenitoba-Johnson, K., Pagano, M., 2012. Fbxw7alpha- and GSK3-mediated degradation of p100 is a pro-survival mechanism in multiple myeloma. Nat. Cell Biol. 14, 375–385.

Cervellati, C., Bonaccorsi, G., Cremonini, E., Romani, A., Fila, E., Castaldini, M.C., Ferrazzini, S., Giganti, M., Massari, L., 2014. Oxidative stress and bone resorption interplay as a possible trigger for postmenopausal osteoporosis. Biomed. Res. Int. 2014, 569563.

Chang, J., Wang, Z., Tang, E., Fan, Z., McCauley, L., Franceschi, R., Guan, K., Krebsbach, P.H., Wang, C.Y., 2009. Inhibition of Osteoblast Functions by IKK/NF-κB in Osteoporosis. Nat. Med. 6, 682–689.

Guillerminet, F., Beaupied, H., Fabien-Soulé, V., Blais, A., 2010. Hydrolyzed collagen improves bone metabolism and biomechanical parameters in ovariectomized mice: an in vitro and in vivo study. Bone 46, 827–834.

Hamada, Y., Fujii, H., Fukagawa, M., 2009. Role of oxidative stress in diabetic bone disorder. Bone 45 (Suppl. 1), S35–S38.

Hendrickx, G., Boudin, E., Van Hul, W., 2015. A look behind the scenes: the risk and pathogenesis of primary osteoporosis. Nat. Rev. Rheumatol. 11, 462–474.

Huang, Q., Gao, B., Jie, Q., Wei, B.Y., Fan, J., Zhang, H.Y., Zhang, J.K., Li, X.J., Shi, J., Luo, Zh.J., Yang, L., Liu, J., 2014. Ginsenoside-Rb2 displays anti-osteoporosis effects through reducing oxidative damage and bone-resorbing cytokines during osteogenesis. Bone 66, 306–314.

Jimi, E., Fukushima, H., 2016. NF-kappaB signaling pathways and the future perspectives of bone disease therapy using selective inhibitors of NF-kappaB. Clin. Calcium 26, 298–304.

Kadenbach, B., Ramzan, R., Vogt, S., 2009. Degenerative diseases, oxidative stress and cytochrome c oxidase function. Trends Mol. Med. 15, 139–147.

Kim, H.K., Kim, M.G., Leem, K.H., 2013. Osteogenic activity of collagen peptide via ERK/MAPK pathway mediated boosting of collagen synthesis and its therapeutic efficacy in osteoporotic bone by back-scattered electron imaging and microarchitecture analysis. Molecules 18, 15474–15489.

Liu, F., Wang, W., Zhang, H., Han, Y.T., Wang, C.B., 2016. Knockdown of REV7 inhibits breast cancer cell migration and invasion. Oncol. Res. 24, 315–325.

Liu, J.L., Zhang, B., Song, S.J., Ma, M., Si, S.Y., Wang, Y.H., Xu, B.X., Feng, K., Wu, J.G., Guo, Y.C., 2014. Bovine collagen peptides compounds promote the proliferation and differentiation of MC3T3-E1 pre-osteoblasts. PLoS One 9, e99920.

Manolagas, S.C., 2010. From estrogen-centric to aging and oxidative stress: a revised perspective of the pathogenesis of osteoporosis. Endocr. Rev. 31, 266–300.

Seo, Y., Hidefumi, F., Maruyama, T., Kuroishi, K., Osawa, K., Nagano, K., Aoki, K., Weih, F., Doi, T., Zhang, M., Ohya, K., Katagiri, T., Hosokawa, R., Jimi, E., 2012. Accumulation of p100, a precursor of NF-kappaB2, enhances osteoblastic differentiation in vitro and bone formation in vivo in aly/aly mice. Mol. Endocrinol. 26, 414–422.

Soysa, N., Alles, N., Weih, D., Lovas, A., Mian, A., Shimokawa, H., Yasuda, H., Weih, F., Jimi, E., Ohya, K., Aoki, K., 2010. The pivotal role of the alternative NF-kappaB pathway in maintenance of basal bone homeostasis and osteoclastogenesis. J. Bone Miner. Res. 25, 809–818.

Thacker, G., Kumar, Y., Parvez Khan, M., Shukla, N., Kapoor, I., Kanaujiya, J., Lochab, S., Ahmed, S., Sanyal, S., Chattopadhyay, N., Trivedi, A., 2016. Skp2 inhibits osteogenesis by promoting ubiquitin–proteasome degradation of Runx2. Biochim. Biophys. Acta 1863, 510–519.

Ueno, T., Yamada, M., Igarashi, Y., Ogawa, T., 2011. N-acetyl cysteine protects osteoblastic function from oxidative stress. J. Biomed. Mater. Res. A 99, 523–531.

Wauquier, F., Leotoing, L., Coxam, V., Guicheux, J., Wittrant, Y., 2009. Oxidative stress in bone remodelling and disease. Trends Mol. Med. 15, 468–477.

Yamazaki, M., Fukushima, H., Shin, M., Katagiri, T., Doi, T., Takahashi, T., Jimi, E., 2009. Tumor necrosis factor alpha represses bone morphogenetic protein (BMP) signaling by interfering with the DNA binding of Smads through the activation of NF-kappaB. J. Biol. Chem. 284, 35987–35995.

Yumimoto, K., Matsumoto, M., Onoyama, I., Imaizumi, K., Nakayama, K.I., 2013. F-box and WD repeat domain-containing-7 (Fbxw7) protein targets endoplasmic reticulum-anchored osteogenic and chondrogenic transcriptional factors for degradation. J. Biol. Chem. 288, 28488–28502.

Zhu, W., He, X.Y., Hua, Y., Li, Q., Wang, J.Y., Gan, X.Q., 2017. The E3 ubiquitin ligase WWP2 facilitates RUNX2 protein transactivation in a mono-ubiquitination manner during osteogenic differentiation. J. Biol. Chem. 292, 11178–11188.